Novel and naturally derived Hydroxyapatite/cellulose nanofibre/curcumin biocomposite for tissue engineering applications

Sridevi S
Periyar University
Ramya S
Central University of Tamil Nadu
Kavitha L
Central University of Tamil Nadu
Gopi Dhanaraj (dhanaraj_gopi@yahoo.com)
Periyar University

Research Article

Keywords: Cellulose nanofibre, Hydroxyapatite, Curcumin, Composite, tissue engineering application

Posted Date: March 18th, 2021

DOI: https://doi.org/10.21203/rs.3.rs-332070/v1

Abstract

Hydroxyapatite (HAp) based composite materials are attaining increasing interest as a potential therapeutic agent for tissue engineering application. In the present study, HAp based composite material is synthesized from biowaste in a cost effective way. Fish bone derived HAp is combined with a cellulose nanofibre (CNF) and curcumin (Cur) as a composite for enhanced thermal, biological and mechanical properties. The HAp/CNF/Cur composite is prepared with different concentrations of CNF (1–3.wt%) and Cur (0.5–1.5 wt%), respectively. Different characterization techniques like Fourier transform-infrared spectroscopy (FT-IR), X-ray diffraction (XRD), Field-emission scanning electron microscopy (FESEM), energy dispersive X-ray (EDX) and thermal gravimetric (TGA) analysis were engaged to assess the functional groups, phase composition, morphology, elemental composition and thermal analysis of the composite. The mechanical strength of the composite is examined using Vickers micro-hardness test. In addition, antibacterial nature of the composite is evaluated against negative and positive bacteria. The viability of human osteosarcoma MG 63 cells over the composite is studied at different concentrations of 1, 3, 7, 10 and 15 µg for 24 h of incubation. Overall, the present investigation shows that the as-synthesized HAp/CNF/Cur composite with enhanced thermal, mechanical and biological properties will be a prospective aspirant for tissue engineering therapeutics.

1 Introduction

Bone tissue engineering is considered as one of the most innovative biomedical technology in the reconstruction and repair of injured tissues linked with tumor resections, osteoporosis, cancer, trauma, or/and infections/inflammation[1, 2]. For this purpose, there is an emergency demand for developing bioceramic material that can assist the regeneration of tissues.[3]

In this point of view, different types of bioceramic materials are being developed and utilized for tissue engineering applications. Among these materials, HAp has attracted considerable attention, and also established to be a prospective bone substitute bioceramic materials [4, 5] due to the numerous essential advantages such as high bioactivity, excellent biocompatibility, osteoconductivity and non toxicity,[6] etc. In addition to this, HAp is an essential candidate because it can form a direct bond with natural bone owing to its resemblance with the mineral fraction of natural bone in chemical and crystallographic structure with living tissues [7].

Different preparation method such as co-precipitation, hydrothermal, sol-gel, ultrasonication and heat treatment has been tailored for HAp synthesis [8–11]. Nowadays, young scientists have mostly focused on the preparation of pure HAp from the biowaste material. Because, then the readily available HAp is very costly owing to the usage of analytical reagents in the synthesis of HAp. As a result, researchers across the world are progressively searching an alternative means toward cost reduction by utilizing some kinds of natural waste materials using the concepts of “waste to wealth” [12]. This great idea gives a novelty to generate a new and safe valuable product from the biowaste material. In addition, these materials can be converted into more precious things which maintains environment safe [13].

Recently, HAp has been synthesized from the biogenically waste material such as fish bone, bovine bone, egg shells and sea shells, etc.[14–17] Due to some resemblance in chemical contents and commercial HAp, it has been motivated possibility to produce HAp material from fish bones. Therefore, fish bone (biowaste) material was used for the synthesis of HAp and this is one of the best ways to minimize the cost [15, 16]. Hence, fish bone has been used as a raw biomaterial for the synthesis of novel HAp. Generally, it is imperative to note down that owing to the growing use of fish worldwide, considerable quantity of fish waste is being formed every year [17]. Universally about 970–2700 billion tons of fish are caught, in which 450–1000 billion are utilized for human consumptions and the remaining is used for fish oil extraction. Hence, utilization of fish bone material can significantly support sustainable environmental development and reduces the environmental issues.

In particular, fish bones are mainly composed of water, collagen, and connective tissue proteins and the remaining 41–84% of other proteins [4, 18]. There are various series of calcium phosphate salts, which are mainly present in fish bone owing to their excellent biological response in physiological environment [12, 13]. Hence, HAp sample was extracted by calcinating the fish bones at various temperatures. Extraction of HAp from fish bone is low cost and biologically safe, since it is easy to obtain [19]. All of these advantages make the as-synthesized HAp from fish bone material more attractive for bone tissue engineering applications [20]. The HAp exhibits low mechanical strength and rigidity which may not be appropriate for tissue engineering applications [21]. In this biomedical point of view, material researchers are focusing on the incorporation of commercial reinforcing materials like carbon nano tubes, carbon nanofibre and some oxides, etc., for the enhancement of mechanical properties [22–24]. However, the cost of commercial reinforcing agents is extremely expensive which sometimes limits the research findings [25]. Therefore, recent researchers are seeking alternative methods towards cost reduction of the reinforcing material [26, 27]. For this purpose, scientists mainly focus on the use of agro-wastes to achieve high expensive biomaterials in an environment friendly approach and sustainable way which can be utilized in tissue engineering applications [28]. In the past few decades, some researchers are focusing on probing natural fibers as reinforcement material in pure HAp, such as hemp, bamboo fiber, jute and kenaf, which were mainly united with biomaterials, so as to find a novel variety of completely bioactive “green composite” [29].

Among various types of polysaccharides such as alginate, cellulose and chitosan possess several advantages like excellent biocompatibility, noncytotoxicity and biodegradability [30]. Generally, cellulose is superior recognized as renewable, biodegradable, biocompatible, thermal stability, environmental friendly biomaterial and non-edible low cost source, representing one of the abundant natural polymer material on earth. Nowadays, cellulose nanofibre (CNF) derived from natural cellulosic sources, are being increasingly examined owing to their special properties [31, 32]. In addition, most CNF have attracted vital significance in tissue engineering applications due to their nanoscale dimensions, low density, high aspect ratio and mainly impressive biological, mechanical and thermal properties. All of these properties make HAp/CNF composite highly attractive for bone tissue engineering applications. Since there is no diverse bioceramic material obtainable to fulfill all the required needs in the biological field, development of biocomposites as a preferred method for biomedical applications has become mandatory [33]. Hence,

the incorporation of bone-bioceramic component of HAp into the CNF has revealed superior interaction and better mechanical properties [34]. This HAp/CNF composite is used in biological process confirms poor antibacterial properties which cannot be appropriate for bone tissue engineering applications.

Curcumin (Cur) is a more active yellow material from Curcuma longa L., which is commonly employed as a flavoring agent and coloring in herbal medicine and food industry in Asian countries to cure the diarrhea, vomiting, headache etc. Generally, curcumin is very safe and healthy product to human and is extensively used for treating Alzheimer's, cystic fibrosis and malarial diseases [35–38]. Based on these positive points, we have concluded that the curcumin could enhance the antibacterial property of the HAp/CNF composite, and thus, a novel biocompatible trinary HAp/CNF/Cur composite is achieved. A composite of HAp/CNF/Cur is expected to contribute a more positive arrangement of biological and mechanical properties and also it is a vital role in the area of biomaterial field. However, as far as we know, the HAp/CNF/Cur composite aimed has not been reported yet.

Thus, the present work aims to implement a green and natural benign procedure consisting of HAp/CNF/Cur composite to deliver enhanced thermal, biological and mechanical properties, so as to provide as a potential applicant for bone tissue engineering applications.

2 Materials And Methods

2.1 Materials

Fresh fishes (Tilabia- Oreochromisniloticus), bamboo fiber and rhizome of curcuma longa were used for the preparation of HAP, CNF and Cur, respectively. Commercially available sodium nitrite ($NaNO_2$), nitric acid (HNO_3), phosphoric acid (H_3PO_4), ethanol (C_2H_5OH), sodium hydroxide (NaOH) and acetic acid (CH_3COOH) were purchased from Sigma-Aldrich chemicals (Aldrich, India). All other chemicals and reagents were obtained from Aldrich, India, as analytical grades. Also, deionized water (DI) was used for the synthesis of the composite.

2.2 Synthesis of HAp, CNF and HAp/CNF/Cur Composite

2.2.1 Synthesis of HAp from Tilabia fish

HAp powder was fabricated in the laboratory using Tilabia fish bones, which are considered as biowaste. Raw Tilabia fishes were collected from harbor at Thiruvarur, Tamilnadu, India. Initially, the fishes were washed and boiled in DI to completely eliminate the fleshy materials. Furthermore the fish bones were dried at 100˚ C in hot air oven for an hour to remove unwanted moisture from the fish bones and the synthesis of HAp was adopted with the procedure reported in literature.[6] After that, the as-prepared samples were calcined at different temperatures (400, 700, 800, 900 and 1000^oC) for 2 h to obtain the fish bone derived HAp.

The as-synthesized HAp sample can be utilized for composite preparation and further characterizations.

2.2.2 Synthesis of CNF

CNF sample was synthesized according to the method described in the previous literature report with some modification [39]. In this preparation, the bamboo fibers were soaked in NaOH for 0.5 h at room temperature to eliminate the impurities, and then washed with deionized water. Accordingly, a bamboo fiber was immersed in a 100 ml mixture solution of H_3PO_4 and HNO_3. The mixture of the bamboo fiber sample was entirely soaked, 0.7 and 1.4 % of $NaNO_2$ were respectively added immediately into the above mixture within 20 min. The remaining procedure of CNF was adopted in accordance with literature report. After removal of the undissolved filtrate, the CNF was finally washed several times with acetone and dried for about 35 min at

60˚ C and then ground into a fine powder which can be used for the preparation of composites and characterizations.

2.2.3 Extraction of curcumin

The rhizome of curcuma longa was harvested from Salem, Tamilnadu, India. After collection of the samples, fresh rhizomes of curcuma longa were directly kept in shed, washed with DI. Subsequently, they were shredded into small threads and then equipped for final curcumin extraction which can be employed for the preparation of the composite. The above extraction was carried out according to the literature report [36].

2.3 Synthesis of Composite

2.3.1 Synthesis of HAp/CNF Composite

A composite of HAp/CNF was synthesized in the 1 wt.% of HAp and different weight percentage of CNF (1–3 wt.%) were dispersed in ethanol-water mixture by using ultrasonication process (Ultrasonicator (EN-60US (Microplus) at 150 W and the frequency of 28 kHz). A cycle of HAp/CNF composite with the appropriate weight ratios of 1:1, 1:2 and 1:3 was synthesized, which was denoted as HAp/CNF-1, HAp/CNF-2 and HAp/CNF-3, respectively. The obtained mixture is exposed to ultrasonic treatment at 2 h in order to ensure a clear distribution of the CNF. Finally, the as-synthesized samples were filtered and dried for 8 h at 60 ˚C and then were ground to fine powder, which can be used for the further preparation of HAp/CNF composite.

2.3.2 Synthesis of HAp/CNF/Cur Composite

The HAp/CNF/Cur sample was prepared by the known quantity of HAp, optimum concentration of CNF and 0.5, 1.0 and 1.5 wt.% of Cur in 40 mL of ethanol-water mixture.

A sequence of HAp/CNF/Cur composite weight ratios of 1:1:0.5, 1:2:1 and 1:3:1.5 was synthesized, which was designated as HAp/CNF/Cur-1, HAp/CNF/Cur-2 and HAp/CNF/Cur-3. This mixture was stirred and ultrasonicated at 2 h for ensuring clear distribution. This final mixture was stirred and ultrasonicated at

room temperature for about 2 h to an effective dispersion. Finally washed with DI, filtered and dried at 80 ˚C for 12 h.

2.4 Chemical and Morphological Characterizations

FT-IR instrument was used to record the curves for the identification of functional groups in the as prepared HAp, HAp/CNF-1, HAp/CNF-2, HAp/CNF-3, HAp/CNF/Cur-1,

HAp/CNF/Cur-2 and HAp/CNF/Cur-3 composite samples.

The diffraction angles of the as synthesized HAp, HAp/CNF-1, HAp/CNF-2, HAp/CNF-3, HAp/CNF/Cur-1, HAp/CNF/Cur-2 and HAp/CNF/Cur-3 composite samples were examined and compared by XRD. The surface morphological nature of the as synthesized HAp, HAp/CNF-1, HAp/CNF-2, HAp/CNF-3 and HAp/CNF/Cur-3 composite samples was studied using FESEM (ZESS). Also, elemental composition of the as prepared sample was investigated using energy dispersive X-ray analysis (EDAX) to identify the elements in the HAp/CNF/Cur-3 composite.

The thermal behavior of the HAp, HAp/CNF-3 and HAp/CNF/Cur-3 composite samples were examined by TGA (Perkin Elmer, Diamond TG/DTA instruments). The as synthesized samples were heated under nitrogen atmosphere in air from 28°C to 700°C.

2.5 Vickers micro-hardness tests

The micro indentation measurements for the HAp, HAp/CNF-1, HAp/CNF-2, HAp/CNF-3 and HAp/CNF/Cur-3 samples were estimated using Vicker diamond intenter (HMV2T, Shimadzu) at room temperature. The Vickers micro-hardness (Hv) measurements were calculated for each of the sample by taking average of five measurements made at five different locations.

2.5.1 Statistical analysis

All trials were triplicate. The one way analysis of variance (ANOVA) was used for statistical analyzing tool utilizing Tukey's test for a post hoc examination. The difference examined between samples was assigned to be significant at $P < 0.05$. Also, all the measured values are presented with ‘*’ so as to convey that significant difference has been calculated.

2.6 Biological Characterizations

2.6.1 Antibacterial activity

The antibacterial activities of the as synthesized HAp/CNF-2, HAp/CNF/Cur-1, HAp/CNF/Cur-2, HAp/CNF/Cur-3 composite was investigated for the two prokaryotic strains that can cause bone infection, that the composite samples were qualitatively deliberate by a standard disc diffusion method [40]. Generally, the greater parts of the infection in the human bone are caused by the two prokaryotic strains such as Escherichia coli (*E. coli*) and Staphylococcus aureus (*S. aureus*). The synthesized

HAp/CNF-2, HAp/CNF/Cur-1, HAp/CNF/Cur-2, HAp/CNF/Cur-3 composite samples was all the discs (6 mm) were equipped from Whatman no: 3 filter paper, which was placed at equal distances after immersing into different concentration of (25, 50, 75, 100, 125 µL) HAp/CNF-2, HAp/CNF/Cur (1–3) samples at 37 ˚C overnight in a incubation chamber. Finally, the zone of inhibition (mm) around the disc of the as synthesized composite was calculated to observe the antibacterial activity.

2.6.2 Biocompatibility Studies

The *in vitro* cell viability of HAp/CNF/Cur–3 composite sample was evaluated through MTT assay (3-[4, 5-dimethylthiazol-2-yl]-2, 5 diphenyltetrazolium Bromide) for 1, 3, 7, 10 and 15 µg for 24 h. The different volumes of HAp/CNF/Cur-3 composite sample were examined by dissolving 0.25 g of HAp/CNF/Cur composite sample in 2 mL of dimethyl sulphoxide. After one day of incubation, each time, 400 µL of MTT was added to each volume and then reserved in incubation for 4 h at 37°C. Finally the MTT assay was then removed, before evaluating absorbance at 570 nm wavelength on microplate by dimethyl sulfoxide was added to dissolve the formazan crystals, and the ELISA microplate was shaken for 15 min. After that, the percentage of the cell viability of HAp/CNF/Cur composite sample was determined using the following formula:

% Cell viability = [A] test / [A] control x 100.

3 Results And Discussion

3.1 Surface characterisation

3.1.1 FT-IR analysis

The FT-IR spectra of HAp, HAp/CNF-1, HAp/CNF-2, HAp/CNF-3 and HAp/CNF/Cur-1, HAp/CNF/Cur-2 and HAp/CNF/Cur-3 composite are revealed in Fig. 1(a-g). The peaks (Fig. 1(a)) observed at 563 and 600 cm^{-1}, 961 and 474 cm^{-1} and 1030 and 1088 cm^{-1} corresponds to the phosphate (PO_4^{3-}) groups of pure HAp [24]. The peaks at 3570 and 631 cm^{-1} are ascribed to the stretching and bending vibration of the hydroxyl (OH^-) groups. Whereas the broad stretching band at 3000–3700 cm^{-1} is attributed to the water molecule of HAP, respectively. The spectra obtained for HAp/CNF-1, HAp/CNF-2 and HAp/CNF-3 composite were shown in Fig. 1 (b-d). All these spectra (Fig. 1 (b-d)) are the overlapped ones of HAp and CNF units. For instance, the peaks appeared at 870 cm^{-1} (C – O – C) and 2900 cm^{-1} (C – H). Furthermore, a peak at 1427 cm^{-1} (O – CH), as well as the band at 3334 cm^{-1} (O – H) in the CNF unit. The FT-IR spectra (Fig. 1 (b-d)) revealed that the band position of the stretching of O – H group of HAp/CNF composite shifted to lower wave number in contrast to that of pure HAp which might be owing to the hydrogen bonding interaction between HAp and CNF. All these FT-IR peaks revealed the presence of CNF in the HAp/CNF material. Apart from these, the stretching band related to the phenolic –OH of Cur at 3570 cm^{-1}, 1599 cm^{-1} (C = O), 1512 cm^{-1} (C = C) and 808, 855 cm^{-1} (are assigned at bending vibration of C – H alkene group) has been attenuated in the Fig. 1 (e-g). Comparing with those of HAP (Fig. 1a), HAp/CNF (Fig. 1 (b-

d)) and the spectrum of the HAP/CNF/Cur (Fig. 1 (e-g)) demonstrates that neither the characteristic peaks shift nor the new peaks are identified with the incorporation of CNF and Cur, signifying that the HAp/CNF/Cur samples are the combination of these HAp, CNF and Cur compounds without new interfacial chemical bonds.

3.1.2 XRD analysis

Figure 2(a-g) illustrates the XRD patterns of HAp, HAp/CNF-1, HAp/CNF-2, HAp/CNF-3 and HAp/CNF/Cur-1, HAp/CNF/Cur-2 and HAp/CNF/Cur-3. The peak (2θ) values of 25.97°, 31.70°, 32.85°,46.85°, 49.7° and 52.36° were assigned to HAp is clearly evident in Fig. 2 (a) (ICDD card No. 09-0432) and also matches well with the previous report [40, 41]. Besides the diffraction peaks of HAp, the characteristic peaks of HAp/CNF-1, HAp/CNF-2 and HAp/CNF-3 (Fig. 2(b-d)) composite samples was examined and cellulose nanofiber merged small peak at 2θ values of 16.58° and 22.04°. As the CNF concentration is increased (1–3 wt.%), the XRD peaks become slightly broader indicating the decreased crystallinity due to the incorporation of CNF in HAp sample (Fig. 2(b-d)). This poor crystalline nature of the HAP/CNF-3 supports improved new bone formation. In addition to these diffraction peaks, the patterns for HAp/CNF/Cur composite samples in Fig. 2 (e-g), exhibited the merged peaks close to 12.28 ^{o} and 17.22^{o} which can be assigned to the diffraction of curcumin. As a result, the HAp/CNF/Cur-3 composite sample illustrates that no appreciable diffraction peaks were formed or lost in the HAp/CNF/Cur-3 composite.

3.3 FESEM and EDAX analysis

The FESEM morphology variation of the as-synthesized HAp, HAp/CNF-1, HAp/CNF-2, HAp/CNF-3 and HAp/CNF/Cur-3 composite samples are revealed in Fig. 3(a-e). The FESEM morphology of the HAp (Fig. 3(a)) revealed granular particles with some agglomerated structure. The morphology of the HAp/CNF sample at three different concentrations of CNF (1, 2 and 3 %) is exhibited in Fig. 3(b-d). The microscopic image of the HAp/CNF-1 sample (Fig. 3(b)) is found to be a needle like rod morphology. Similarly, the morphology for HAp/CNF-2 composite sample exhibited typical needle-like structure (Fig. 3(c)). On further increasing the concentration up to 3 wt.% of CNF (HAp/CNF-3 (Fig. 3(d)), the FESEM image revealed a highly distributed uniform needle like morphology and compact composite. Interestingly, when 1.5 wt.% of Cur is added in HAp/CNF-3 (HAp/CNF/Cur) composite (Fig. 3 (e)), a morphology of compactly organized agglomerated flower like microstructure is obtained with closely packed structure without any voids.

The EDAX spectrum of the HAp/CNF/Cur composite is showed in Fig. 3 (f) which spectrum was strongly evidence the presence of Ca, Mg, P, C and O elements. The EDAX spectrum which is confirmed the presence of chemical elements in the composite like calcium, phosphorous and magnesium typical of HAp phase, carbon and oxygen representative of CNF and Cur.

3.4 TGA analysis

The TGA analysis of the as-synthesized HAp, HAp/CNF-3 and HAp/CNF/Cur-3 composite samples in nitrogen atmosphere were carried out between 28°C-700°C in air which was aged at a heating rate of

20°C min^{-1} for one day as revealed in Fig. 4 (a-c). As shown from TGA curve on Fig. 4(a), the initial weight loss observed at 100°C is due to the evaporation of water molecule. The weight loss region between 325°C and 450°C is mainly owing to the decomposition of the organic components present in the HAp sample. In case of HAp/CNF-3 sample (Fig. 4(b)), the initial weight loss occurs below 200°C corresponds to the evaporation of adsorbed water. The second stage observed from 250°C and 360°C is possibly due to the decomposition of organic phase, followed by the third stage at around 460°C which is due to the oxidization of decomposition products. It was observed that the HAp/CNF/Cur-3 composite sample (Fig. 4(c) showed a weight loss from 100°C to 128°C owing to the moisture content vaporization. From the Fig. 4(c), it can be seen that the HAp/CNF/Cur-3 sample start to decompose at 206–541°C, while the Cur starts to decompose at 285°C. The temperature at the degradation rate for CNF is about 410°C. The sharp weight loss that could be attributed to the decomposition of HAp/CNF/Cur-3 composite can be related to the incorporation of water molecules and adsorbed solvent. The good thermal stability of HAp/CNF/Cur-3 composite may be owing to the excellent distribution of CNF and Cur in the HAp unit and the strong interaction between these three components. These observation indicating that the as-synthesized HAp/CNF/Cur-3 composite samples exhibit a strong thermal stability which can also be used at temperatures above 600°C.

3.5 Vickers micro-hardness

In the present study, the Vickers micro-hardness values (Hv) of the HAp, HAp/CNF-1, HAp/CNF-2, HAp/CNF-3 and HAp/CNF/Cur-3 composite samples are represented in Fig. 5. It is seen from the figure, the Hv value observed for the HAp/CNF/Cur-3 composite was found to be 69.1 Hv, which results was higher than that of the HAp, HAp/CNF-1, HAp/CNF-2 and HAp/CNF-3 (52.0, 54.5, 67.75 and 50.1 Hv), respectively. Finally, the obtained results it is noticeable that the presence of CNF plays an important role in enhancing the mechanical property of the composite, which will be more beneficial in bone tissue engineering applications.

3.6 Biological Characterizations

3.6.1 Antibacterial activity

In vitro activity of the as-synthesized HAp/CNF-3, HAp/CNF/Cur-1, HAp/CNF/Cur-2 and HAp/CNF/Cur-3 composite samples have been investigated by using the agar disc diffusion method. The two prokaryotic strains (such as *E. coli* and *S. aureus*) are the universal bacteria that are mainly found in the contaminated wound [41]. The HAp/CNF-3, HAp/CNF/Cur-1, HAp/CNF/Cur-2 and HAp/CNF/Cur-3 composite samples were tested against two prokaryotic strains at five various concentrations such as 25, 50, 75, 100 and 125 µL as illustrated in Fig. 6. When compared to HAp/CNF-3, HAp/CNF/Cur-1, HAp/CNF/Cur-2 and HAp/CNF/Cur-3 composites, the HAp/CNF/Cur-3 composite sample exposed improved antibacterial activity which is strongly validated from the zone of inhibition (Fig. 6). The activity results are very well supported by the measured inhibition zone for the optimum and highest concentration (1.5 wt%) of Cur in HAp/CNF/Cur composite against the two bacteria, which were found to be the zone of inhibition 5, 6, 6, 8, and 9 mm for *S. aureus*, and 6, 10, 10, 12, and 13 mm for *E. coli*,

respectively. In general, the antibacterial activity of HAp/CNF/Cur-3 composite sample against *E. coli* strain was fairly superior when compared to that of *S. aureus* strain and also it indicates the HAp/CNF/Cur-3 composite is more active against *E. coli* strain which suggesting more effective and excellent antibacterial activity.

3.6.2 *In vitro* Cell viability test

The *in vitro* cell viability of HOS MG63 cells on the HAp/CNF/Cur-3 (at optimum concentration of Cur (1.5 wt.%)) composite sample is showed in Fig. 7. The bright filed images of the HAp/CNF/Cur-3 composite sample at 1, 3, 7, 10 and 15 µg in cultured medium are exposed in Fig. 7 (a-f). It can be obviously noticed from the Fig. 7 (b-f), the increase quantity of viable cells was seen in the HAp/CNF/Cur-3 composite sample. The composite (HAp/CNF/Cur-3) sample at 15 µg incubation of culture medium (Fig. 7(f)) exhibits the occurrence of larger amount of viable cells which strongly confirms that the excellent biocompatibility of the HAp/CNF/Cur-3 composite sample has been enhanced by the presence of both CNF and Cur at optimum concentration of 2 and 1.5.wt%, respectively in the sample. Finally, the viability results showed that the HAp/CNF/Cur-3 composite sample exhibited superior promotion of the *in vitro* cell viability which is more supporting for the tissue engineering applications.

4 Conclusions

In this present study, a novel approach was adopted to synthesize a HAp/CNF/Cur-3 composite from biowaste material. The structural and morphological characterization clearly exhibited the formation of HAp/CNF/Cur-3 composite which is clearly evident from the FT-IR, XRD and FESEM. The resulting HAp/CNF/Cur-3 composite showed excellent mechanical strength owing to the presence of CNF. Furthermore, the presence of CNF and Cur in HAp/CNF/Cur-3 composite increased the thermal properties. The presence of Cur in the as-synthesized material revealed the good antibacterial activity against the *E. coli* and *S. aureus*. More importantly, the as-synthesized HAp/CNF/Cur-3 composite induced excellent biocompatibility *in vitro*. Therefore, the as-synthesized HAp/CNF/Cur-3 composite material exhibits the significance of vital potential components for bone tissue engineering owing to their excellent thermal, biocompatibility and antibacterial properties along with improved mechanical properties.

Declarations

Acknowledgements

Prof. D. Gopi acknowledges the major financial support from the Department of Science and Technology (DST-SERB, Ref. No.:EMR/2017/003803) and University Grants Commission (UGC) (Ref. No. CSR-KN/CRS-118/2018-19/1056, Dated: 26.12.2018). One of the authors

References

1. Selvakumar M, Pawar HS, Francis NK et al (2016) Excavating the Role of Aloe Vera Wrapped Mesoporous Hydroxyapatite Frame Ornamentation in Newly Architectured Polyurethane Scaffolds for Osteogenesis and Guided Bone Regeneration with Microbial Protection. ACS Appl Mater Interfaces 8:5941–5960
2. Gao X, Song J, Ji P, Zhang X et al (2016) Polydopamine-Templated Hydroxyapatite Reinforced Polycaprolactone Composite Nanofibers with Enhanced Cytocompatibility and Osteogenesis for Bone Tissue Engineering. ACS Appl Mater Interfaces 8:3499–3515
3. Hk Xu H, Wang P, Wang L et al (2017) Calcium phosphate cements for bone engineering and their biological properties. Bone Res 5:17056
4. Gopi D, Kanimozhi K, Bhuvaneshwari N et al (2014) Novel banana peel pectin mediated green route for the synthesis of hydroxyapatite nanoparticles and their spectral characterization. Spectrochim Acta A 118:589–597
5. Gopi D, Shinyjoy E, Kavitha L (2014) Synthesis and spectral characterization of silver/magnesium co-substituted hydroxyapatite for biomedical applications. Spectrochim Acta Part A 127:286–291
6. Pal A, Paul S, Choudhury AR et al (2017) Synthesis of hydroxyapatite from Lates calcarifer fish bone for biomedical applications. Mater Lett 203:89–92
7. Anwar A, Rehman IU, Darr JA (2016) Low-Temperature Synthesis and Surface Modification of High Surface Area Calcium Hydroxyapatite Nanorods Incorporating Organo functionalized Surfaces. J Phys Chem C 120:29069–29076
8. Inan T, Komur B, Ekren N et al (2017) Physical Characterization of Turbot (Psetta Maxima) Originated Natural Hydroxyapatite. Acta Phys Pol 131:397–400
9. Gopi D, Nithiya S, Shinyjoy E, Kavitha L (2012) Spectroscopic investigation on formation and growth of mineralized nanohydroxyapatite for bone tissue engineering applications. Spectrochim Acta Part A 92:194–200
10. Gopi D, Ramya S, Rajeswari D et al (2014) Strontium, cerium co- substituted hydroxyapatite nanoparticles: Synthesis, characterization, antibacterial activity towards prokaryotic strains and *in vitro* studies. Colloids Surfaces A: Physicochem Eng Aspects 451:172–180
11. Gopi D, Indira J, Kavitha L et al (2012) Synthesis of hydroxyapatite nanoparticles by a novel ultrasonic assisted with mixed hollow sphere template method. Spectrochim Acta Part A 93:131–134
12. Anjaneyulu U, Pattanayakand DK, Vijayalakshmi U (2016) Snail Shell Derived Natural Hydroxyapatite: Effects on NIH-3T3 Cells for Orthopedic Applications. Mater Manuf Process 31:206–216
13. Khoo W, Nor FM, Ardhyananta H et al (2015) Preparation of Natural Hydroxyapatite from Bovine Femur Bones Using Calcination at Various Temperatures. Procedia Manuf 2:196–201
14. Shavandi A, Bekhita AA, Ali A et al (2015) Synthesis of nano-hydroxyapatite (nHA) from waste mussel shells using a rapid microwave method. Mater Chem Phys 149–150:607–616

15. Hassan MN, Mahmoud MM, Link MM (2016) G, et al. Sintering of naturally derived hydroxyapatite using high frequency microwave processing. J Alloy Compd 682:107–114
16. Mustafa N, Ibrahim MHI, Asmawi R et al (2015) Hydroxyapatite extracted from Waste Fish Bones and Scales via Calcination Method. Appl Mech Mater 773–774:287–290
17. Yamamura H, Silva VHP, Ruiz PLM et al (2018) Physico-chemical characterization and biocompatibility of hydroxyapatite derived from fish waste. J Mech Behav Biomed Mater 80:137–142
18. Yin T, Park JW, Xiong S (2015) Physicochemical properties of nano fish bone prepared by wet media milling. LWT – Food Sci Technol 64:367–373
19. Mocanu AC, Stan GE, Maidaniuc A et al (2019) Naturally-Derived Biphasic Calcium Phosphates through Increased Phosphorus-Based Reagent Amounts for Biomedical Applications. Materials 12:381
20. Mondal S, Pal U, Dey A (2016) Natural origin hydroxyapatite scaffold as potential bone tissue engineering substitute. Ceram Int 42:18338–18346
21. Zhang L, Zhang C, Zhang R et al (2019) Extraction and characterization of HA/b-TCP biphasic calcium phosphate from marine fish. Mater Lett 236:680–682
22. Rajkumar M, Meenakshisundaram N, Rajendran V (2011) Development of nanocomposites based on hydroxyapatite/sodium alginate: Synthesis and characterization. Mater Lett 62:469–479
23. Guo W, Wang X, Zhang P et al (2018) Nano-fibrillated cellulose-hydroxyapatite based composite foams with excellent fire resistance. Carbohydr Poly 195:71–78
24. Shinyjoy E, Kavitha L, BhagyaMathi D et al (2017) Carbon Nanofiber/Polycaprolactone/Mineralized Hydroxyapatite Nanofibrous Scaffolds for Potential Orthopedic Applications. ACS Appl Mater Interfaces 9:6342–6355
25. Nagalakshmaiah M, El Kissi N, Dufresne A (2016) Ionic Compatibilization of Cellulose Nanocrystals with Quaternary Ammonium Salt and Their Melt Extrusion with Polypropylene. ACS Appl Mater Interfaces 8:8755–8764
26. Park M, Lee D, Shin S et al (2015) Effect of negatively charged cellulose nanofibers on the dispersion of hydroxyapatite nanoparticles for scaffolds in bone tissue engineering. Colloids Surf B Biointerfaces 130:222–228
27. Pelissari FM, Mahecha MMA, Sobral PJDA et al (2017) Nanocomposites based on Banana Starch Reinforced with Cellulose Nanofibers Isolated from Banana Peels. J Colloid Interf Sci 505:154–167
28. Bigliardi SC, Toro RO, Boix AC (2018) Isolation and characterisation of microcrystalline cellulose and cellulose nanocrystals from coffee husk and comparative study with rice husk. Carbohydr Poly 191:205–215
29. Jiang L, Li Y, Xiong C et al (2017) Preparation and Properties of Bamboo Fiber/Nano-hydroxyapatite/Poly(lactic-co-glycolic) Composite Scaffold for Bone Tissue Engineering. ACS Appl Mater Interfaces 9:4890–4897

30. Jiang H, Zuo Y, Zou Q et al (2013) Biomimetic Spiral-Cylindrical Scaffold Based on Hybrid Chitosan/Cellulose/Nano-Hydroxyapatite Membrane for Bone Regeneration. ACS Appl Mater Interfaces 5:12036–12044
31. Chen Q, Garcia RP, Munoz J et al (2015) Cellulose Nanocrystals Bioactive Glass Hybrid Coating as Bone Substitutes by Electrophoretic Co-deposition: In Situ Control of Mineralization of Bioactive Glass and Enhancement of Osteoblastic Performance. *ACS Appl Mater Interfaces* Interfaces 7:24715–24725
32. Leite LMP, Zanon CD, Menegalli FC (2017) Isolation and characterization of cellulose nanofibers from cassavaroot bagasse and peelings. Carbohydr Poly 157:962–970
33. Xie J, Hse CY, Hoop CFD, Hu T et al (2016) Isolation and characterization of cellulose nanofibers from bamboo using microwave liquefaction combined with chemical treatment and ultrasonication. Carbohydr Poly 151:725–734
34. Ao C, Niu Y, Zhang X et al (2017) Fabrication and characterization of electrospuncellulose/nano-hydroxyapatite nanofibers for bone tissue engineering. Int J Biol Macromol 97:568–573
35. Liu Z, Huang P, Law S et al. Preventive Effect of Curcumin Against Chemotherapy-Induced Side-Effects. *Front Pharmacol* 2018, 9
36. Nong HV, Hung LX, Thang PN et al (2016) Fabrication and vibration characterization of curcumin extracted from turmeric (Curcuma longa) rhizomes of the northern Vietnam. Springerplus 5:1147
37. Jogiya B, Chudasama K, Thaker V et al (2018) Synthesis and characterization of novel bio-material: Nano composites of hydroxyapatite and curcumin. Int J Appl Ceram Technol 15:148–160
38. Bhawana, Basniwal RK, Buttar HS et al (2011) Curcumin Nanoparticles: Preparation, Characterization, and Antimicrobial Study. J Agric Food Chem 59:2056–2061
39. Xua Y, Liub X, Liuc X et al (2014) Influence of HNO_3/H_3PO_4–$NANO_2$ mediated oxidation on thestructure and properties of cellulose fibers. Carbohydr Poly 111:955–963
40. Sathishkumar S, Kavitha L, Shinyjoy E et al (2016) Tailoring the Sm/Gd-Substituted Hydroxyapatite Coating on Biomedical AISI 316L SS: Exploration of Corrosion Resistance, Protein Profiling, Osteocompatibility, and Osteogenic Differentiation for Orthopedic Implant Applications. Ind Eng Chem Res 55:6331–6344
41. Gopi D, Shinyjoy E, Kavitha L (2015) Influence of ionic substitution in improving the biological property of carbon nanotubes reinforced hydroxyapatite composite coating on titanium for orthopedic applications. Ceram Int 41:5454–5463

Figures

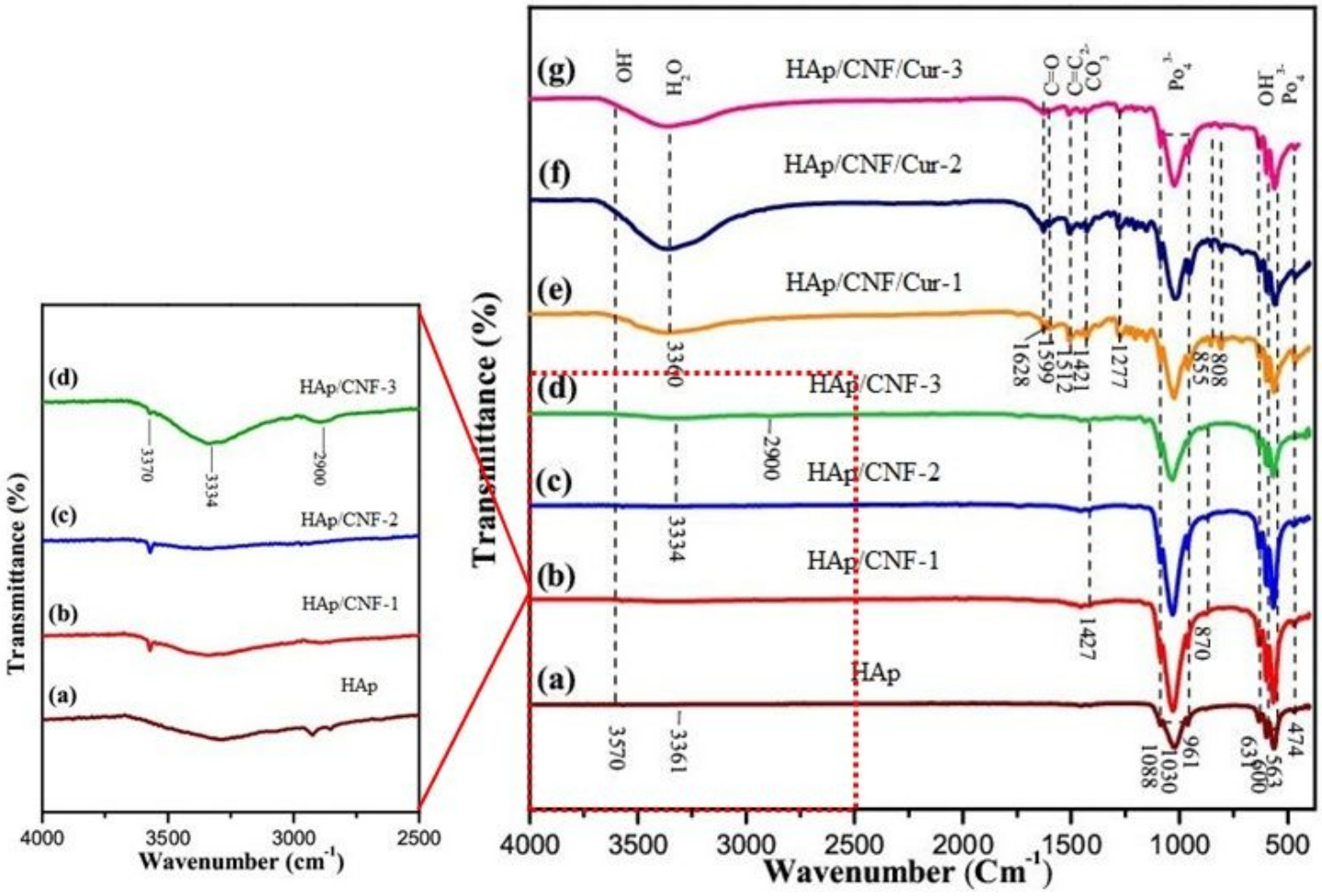

Figure 1

FT-IR spectra for (a) HAp, (b)HAp/CNF-1, (c) HAp/CNF-2, (d) HAp/CNF-3, (e) HAp/CNF/Cur-1, (f) HAp/CNF/Cur-2 and (g) HAp/CNF/Cur-3 composite sample.

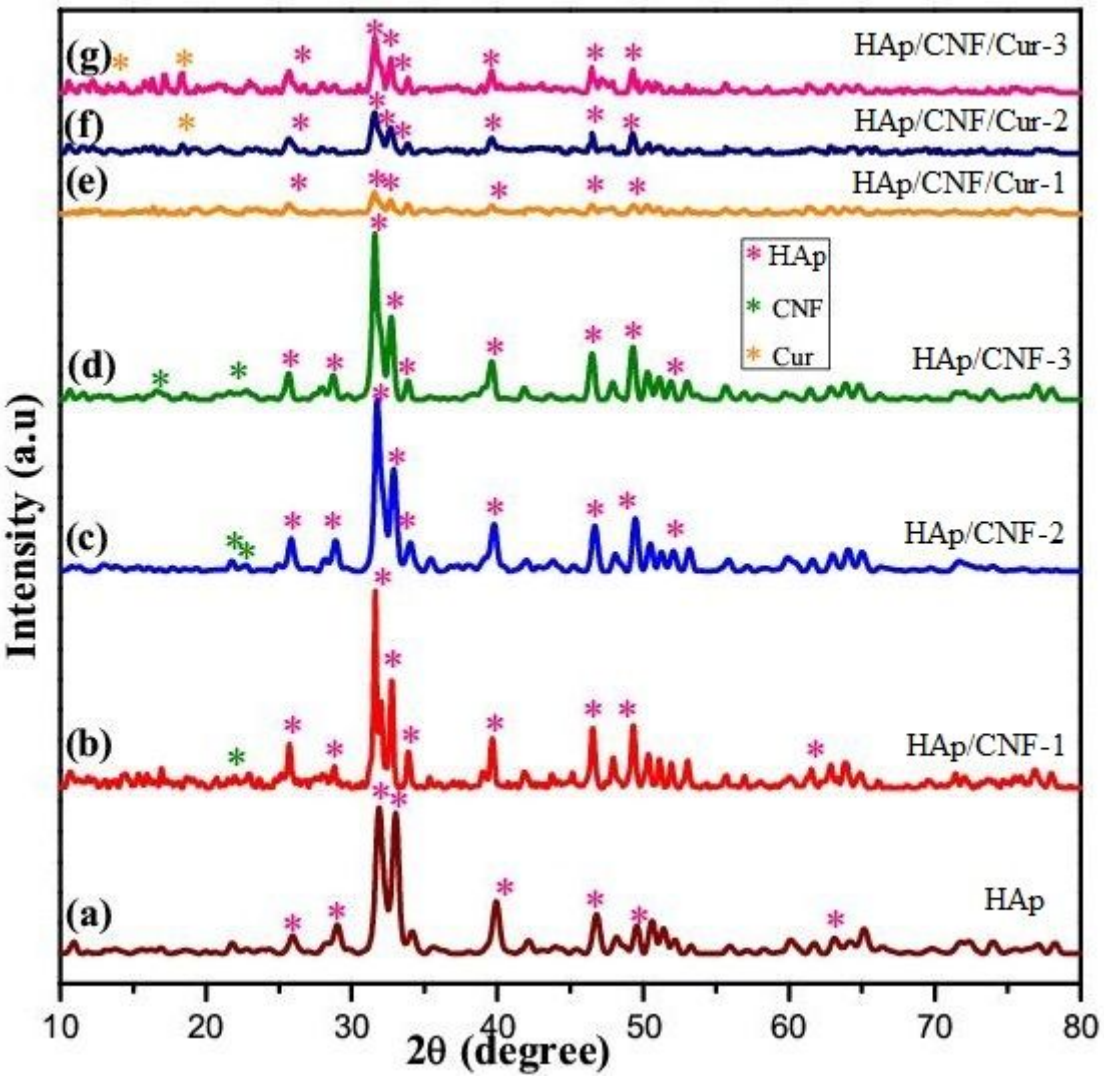

Figure 2

XRD spectra for (a) HAp, (b)HAp/CNF-1, (c) HAp/CNF-2, (d) HAp/CNF-3, (e) HAp/CNF/Cur-1, (f) HAp/CNF/Cur-2 and (g) HAp/CNF/Cur-3 composite sample.

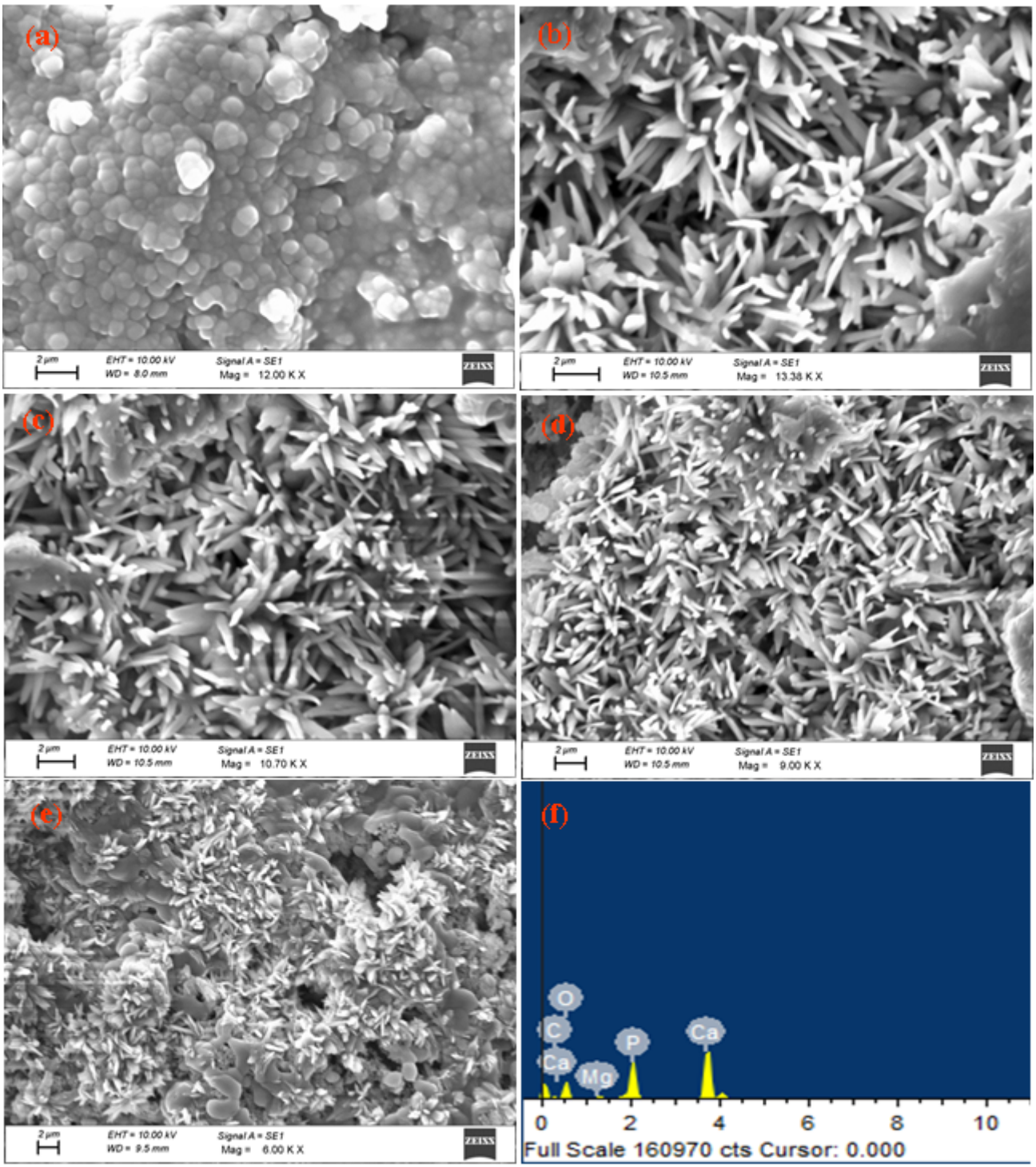

Figure 3

FESEM images of (a) HAp, (b) HAp/CNF-1, (c) HAp/CNF-2, (d) HAp/CNF-3, (e) HAp/CNF/Cur-3 composite and (f) EDAX spectrum of HAp/CNF/Cur-3 composite sample.

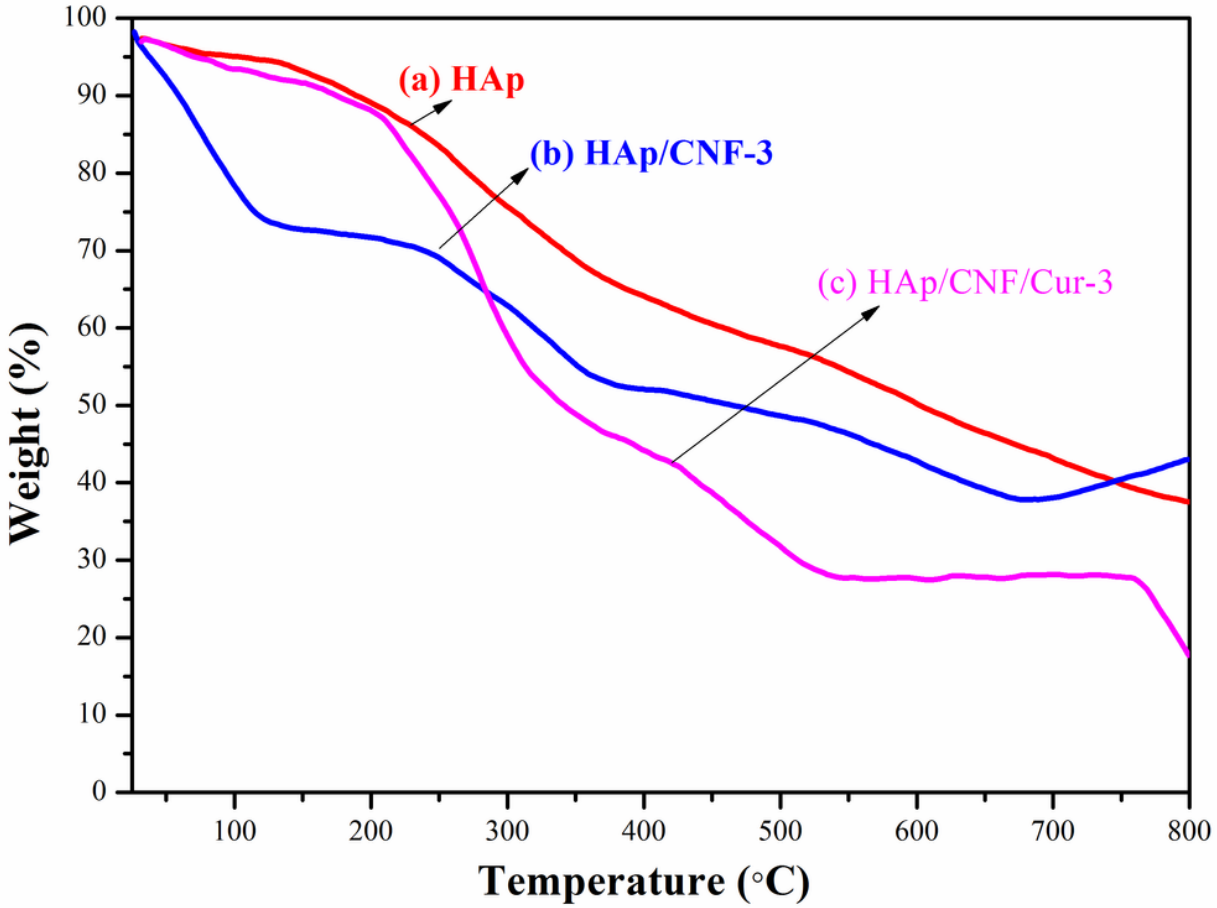

Figure 4

Thermal gravimetric analysis of (a) HAp, (b) HAp/CNF-3 and HAp/CNF/Cur-3 composite sample.

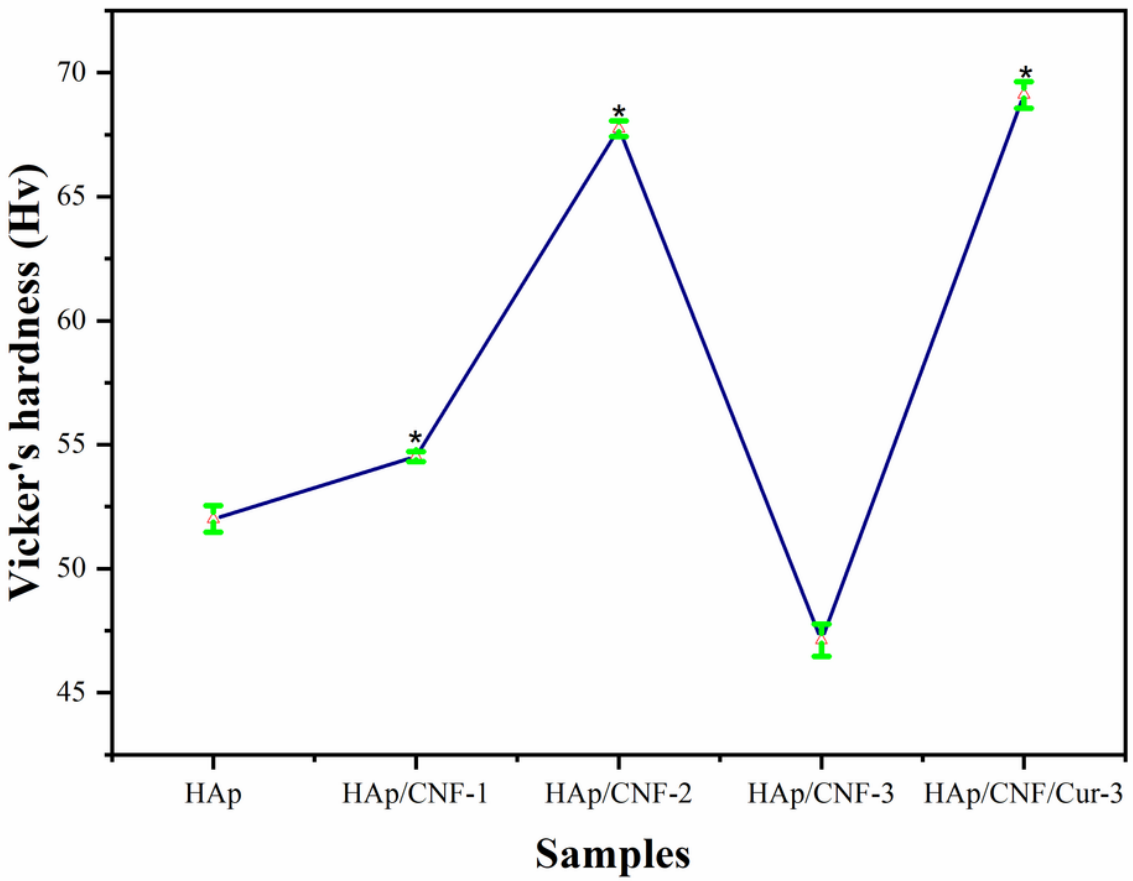

Figure 5

Vickers micro hardness of HAp, HAp/CNF-1, HAp/CNF-2, HAp/CNF-3 and HAp/CNF/Cur composite sample.

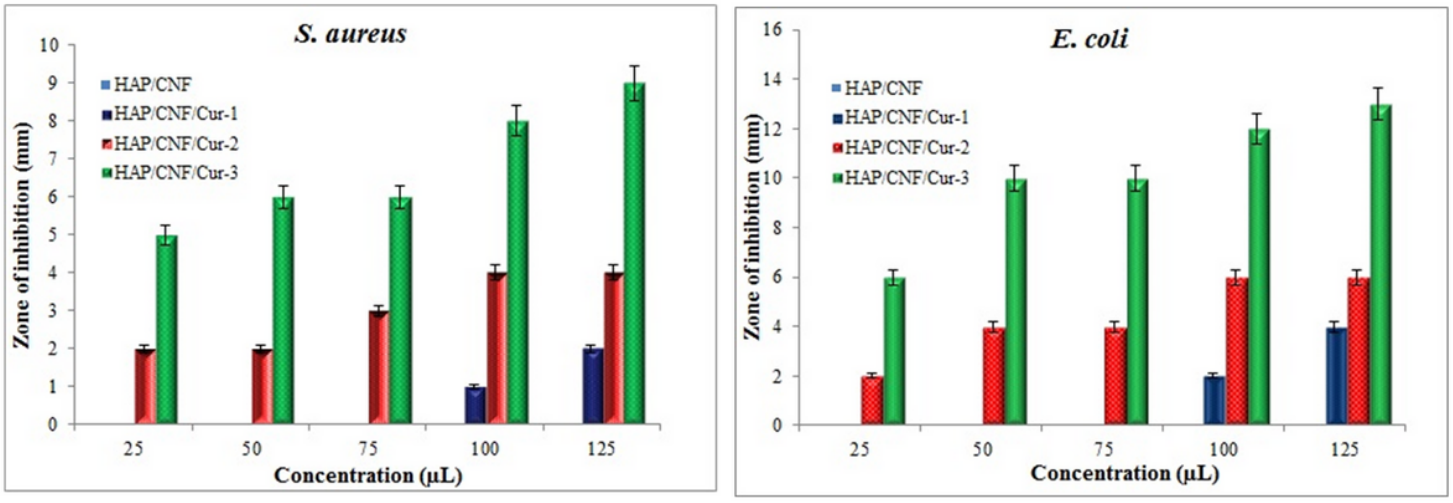

Figure 6

Antibacterial activity of HAp, HAp/CNF, HAp/CNF/Cur-1, HAp/CNF/Cur-2, HAp/CNF/Cur-3 composite sample at different concentrations (25, 50, 75, 100 & 125 µL) against E.coli and S. aureus.

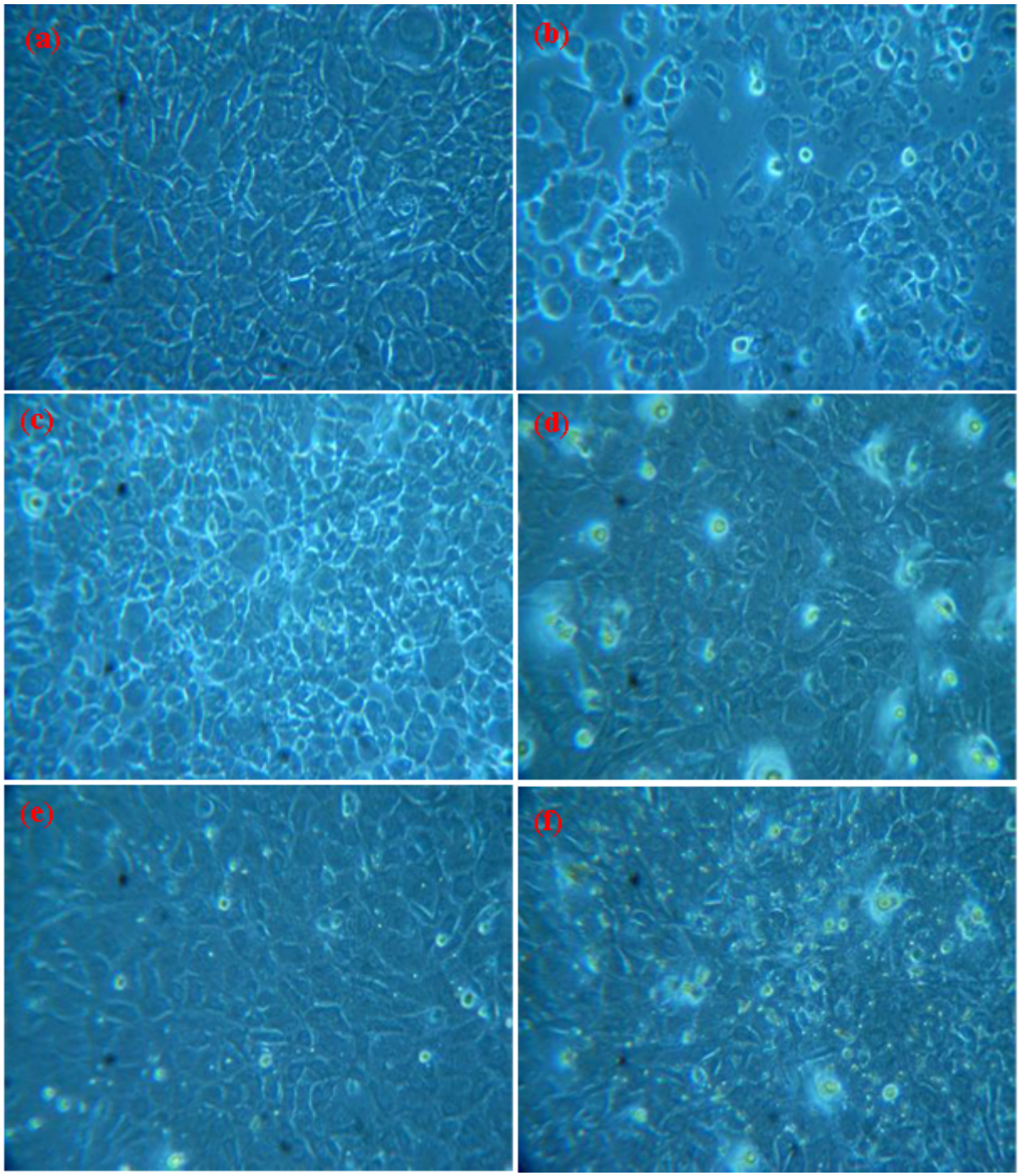

Figure 7

Cell viability of HAp/CNF/Cur-3 composite synthesized sample shows the (a) Control, (b-f) 1, 3,7,10 and 15 µg.

Supplementary Files

This is a list of supplementary files associated with this preprint. Click to download.

- graphicalabstratct.jpg